



Contents lists available at ScienceDirect

Physica C

journal homepage: [www.elsevier.com/locate/physc](http://www.elsevier.com/locate/physc)

## Size effects of nano-scale pinning centers on the superconducting properties of YBCO single grains

Nahed Moutalbi<sup>a,\*</sup>, Jacques G. Noudem<sup>b</sup>, Ali M'chirgui<sup>a</sup>

<sup>a</sup> Systems and Applied Mechanics Laboratory LASMAP, Polytechnic School of Tunisia, Rue El Kawarezi La Marsa 743, Tunis, Tunisia

<sup>b</sup> CRISMAT/CNRS, UCBN/ENSICAEN, 6 Bd Maréchal Juin, 14050 Caen, France

### ARTICLE INFO

#### Article history:

Received 10 January 2014

Received in revised form 12 April 2014

Accepted 16 April 2014

Available online xxxxx

#### Keywords:

Bulk

Pinning

Vortices

### ABSTRACT

High pinning superconductors are the most promising materials for power engineering. Their superconducting properties are governed by the microstructure quality and the vortex pinning behavior. We report on a study of the vortex pinning in  $\text{YBa}_2\text{Cu}_3\text{O}_{7-x}$  (YBCO) single grain with defects induced through the addition of insulating nano-particles. In order to improve the critical current density, YBCO textured bulk superconductors were elaborated using the Top Seeded Melt Texture and Growth process with different addition amounts of  $\text{Al}_2\text{O}_3$  nano-particles. Serving as strong pinning centers, 0.05% excess of  $\text{Al}_2\text{O}_3$  causes a significant enhancement of the critical current density  $J_c$  under self field and in magnetic fields at 77 K. The enhanced flux pinning achieved with the low level of alumina nano-particles endorses the effectiveness of insulating nano-inclusions to induce effective pinning sites within the superconducting matrix. On the other side, we focused on the effect of the size of pinning centers on the critical current density. This work was carried out using two batches of alumina nano-particles characterized by two different particle size distributions with mean diameters  $\text{PSD}_1 = 20 \text{ nm}$  and  $\text{PSD}_2 = 2.27 \mu\text{m}$ . The matching effects of the observed pinning force density have been compared. The obtained results have shown that the flux pinning is closely dependent on the size of the artificial pinning centers. Our results suggest that the optimization of the size of the artificial pinning centers is crucial to a much better understanding of the pinning mechanisms and therefore to insure high superconducting performance for the practical application of superconducting materials.

© 2014 Published by Elsevier B.V.

### 1. Introduction

Following the discovery of high temperature superconductors (HTS) materials, research on their applications has drawn much more attention. Their various applications are crucially dependent on their critical current density ( $J_c$ ) [1,2]. Indeed, the large scale application of (RE)-BCO materials is contingent upon achieving both high inter-granular critical current density by grain texturing and high intra-granular critical current density by flux pinning. To eliminate the weak links, great progress has been made by the development of various forms of melt texture and growth process [3–7]. The continuous material improvement has resulted to higher  $J_c$  values [3–7]. However, the aptitude of HTS materials to carry currents is drastically dropped in the presence of magnetic fields. Impressive efforts have been spent in improving the critical current density ( $J_c$ ) in bulk superconductors by the addition of nano-sized inclusions which can work as effective pinning sites

for vortices [8–10]. Several types of nano-sized inclusions, such as  $\text{ZrO}_2$ ,  $\text{SnO}_2$ ,  $\text{ZnO}$  and  $\text{BaZrO}_3$ , have been reported to serve as efficient pinning sites resulting in enhancements in flux pinning and thus in the critical current density ( $J_c$ ) [5,10–13]. Moreover, it was reported that  $(\text{RE})_2\text{-B}_1\text{C}_1\text{O}_5$  secondary phase resulted from the incomplete peritectic recombination of (RE)-BCO phase is considered to be another effective flux pinning center resulting in improvement in  $J_c$  behavior [8,14,15]. In spite of all these efforts, the flux pinning progress in HTS materials remain a very complex phenomenon which is not amply understood. The leading mechanisms of pinning induced by both nano-sized inclusions and  $(\text{RE})_2\text{-B}_1\text{C}_1\text{O}_5$  precipitates remain unrevealed because of their size which is larger than the coherence length  $\xi$ . It was generally believed that the optimal size of a pinning center should be comparable to the coherence length  $\xi$  [16]. By contrast, theoretical reports suggest that the optimal size of efficient pinning center should be comparable to the size of the penetration depth  $\lambda$  rather than the size of the coherence length  $\xi$  [17–20]. For these reasons, understanding the mechanisms behind the dependence of  $J_c$  on the

\* Corresponding author. Tel.: +216 72 591 906.

E-mail addresses: [nahed.moutalbi@yahoo.fr](mailto:nahed.moutalbi@yahoo.fr), [nahedbiz@yahoo.fr](mailto:nahedbiz@yahoo.fr) (N. Moutalbi).

size of the pinning center is a crucial way to optimize the properties of superconducting materials.

In this work, the emphasis was focused on the effect of the addition of nano-sized inclusions of  $\text{Al}_2\text{O}_3$  on the superconducting properties. The influence of the size of the pinning centers on the pinning strength was also reported.

## 2. Experimental details

YBaCuO single grain bulk samples were synthesized from commercial precursors  $\text{Y}_2\text{Ba}_1\text{Cu}_1\text{O}_5$  (Y211),  $\text{Y}_1\text{Ba}_2\text{Cu}_3\text{O}_{7-x}$  (Y123),  $\text{SnO}_2$  and  $\text{CeO}_2$  with an initial composition of Y123 + 25 mol.% Y211 + 0.5 wt.%  $\text{CeO}_2$  + 0.25 wt.%  $\text{SnO}_2$ . The doping with  $\text{Al}_2\text{O}_3$  nano-inclusions was realized with the addition of various amounts ranging from 0.01 wt.% to 0.1 wt.%. Two batches of  $\text{Al}_2\text{O}_3$  nano-inclusions with different particle size distributions were used. Powders were thoroughly mixed by ball milling in order to homogenize the powders and then pressed into pellets of 16 mm in diameter. The preforms were isolated from the  $\text{Al}_2\text{O}_3$  substrate by a bed of  $\text{Yb}_2\text{O}_3/\text{Y}_2\text{O}_3$  powders. A cold seeding process was employed by the use of SmBaCuO seed. The preforms were heated to 1045 °C and held at this temperature for 2 h, cooled to 1025 °C for 0.4 h. The cooling to 986 °C was at a rate of 2 °C/h and then further slowly cooling was realized at a rate of 0.2 °C/h–975 °C. The cooling to 940 °C was at a rate of 2 °C/h. Finally pellets were furnace cooled to room temperature.

X-ray diffraction measurements were carried out using  $\text{Cu K}\alpha$  radiation to confirm the orientation. Superconducting properties were measured with a Quantum Design Superconducting SQUID magnetometer. The magnetic  $J_c$  values were deduced from the  $M(H)$  loops on the basis of the extended Bean critical state model [22]  $J_c = 2\Delta M/a(1-a/3b)$ , where  $\Delta M$  is the magnetization hysteresis in  $\text{emu cm}^{-3}$ ,  $a$  and  $b$  are the dimensions of the sample in the plane perpendicular to the applied field.

## 3. Results

Fig. 1 shows the top view of the as-grown YBCO bulk prepared by TSMTG process in air. It can be seen from the picture that the sample of 16 mm in diameter grew in the form of single grain from the seed crystal with clearly fourfold growth facet lines. Similar results were obtained for YBCO bulk samples with addition of  $\text{Al}_2\text{O}_3$  nano-particles. An example of the X-ray diffraction pattern of the top surface of the bulk of YBCO melt-textured single grain with 0.01 wt.% of PSD<sub>1</sub> nano-particles is shown in Fig. 2. Only



Fig. 1. The top view of the as-grown YBCO bulk prepared by TSMTG process in air.

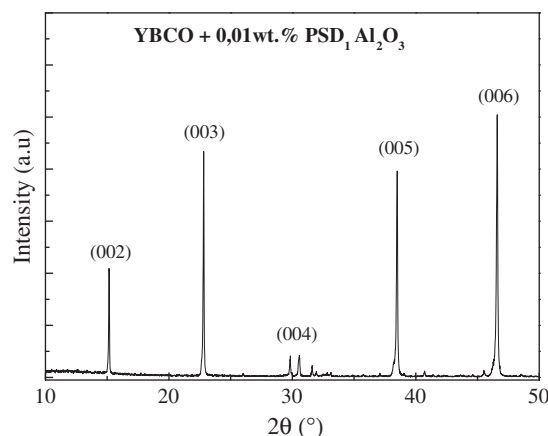


Fig. 2. X-ray diffraction pattern of the top surface of YBCO melt-textured single grain with 0.01 wt.% of PSD<sub>1</sub>  $\text{Al}_2\text{O}_3$  nano-particles.

(001) diffraction peaks were observed indicating the c-axis orientation of the single grain. Similar results were obtained for all the samples fabricated with PSD<sub>1</sub> and PSD<sub>2</sub>  $\text{Al}_2\text{O}_3$  nano-particles.

Fig. 3 shows the  $J_c$  curves versus applied magnetic field for various addition amount of PSD<sub>1</sub> and PSD<sub>2</sub>  $\text{Al}_2\text{O}_3$  nano-particles. The remanent  $J_c$  and the  $J_c$  at intermediate magnetic field is enhanced with the addition of  $\text{Al}_2\text{O}_3$  nano-particles. The  $J_c$  (77 K, 0 T) increases from  $4 \times 10^4 \text{ A cm}^{-2}$  to  $7 \times 10^4 \text{ A cm}^{-2}$  and  $5.7 \times 10^4 \text{ A cm}^{-2}$  for the reference sample and YBCO bulk with 0.01 wt.% and 0.05 wt.% of PSD<sub>1</sub>  $\text{Al}_2\text{O}_3$  nano-particles respectively.

For YBCO bulk with 0.01 wt.% and 0.05 wt.% of PSD<sub>1</sub>  $\text{Al}_2\text{O}_3$  nano-particles  $J_c$  exhibit an enhancement from 0 T to 4 T compared to the reference sample. Such improvement in  $J_c$  can be attributed to the effectiveness of  $\text{Al}_2\text{O}_3$  nano-particles or associated defects to serve as artificial pinning centers within the superconducting matrix. One should note that YBCO bulk with 0.10 wt.% of PSD<sub>1</sub>  $\text{Al}_2\text{O}_3$  nano-particles evinces lower  $J_c$  values in the whole field range. This result stems from the deterioration in superconducting properties due to excess of  $\text{Al}_2\text{O}_3$  addition.

For comparison, we plot in the same Fig. 3b the curves of  $J_c = f(\mu_0 H_a)$  for YBCO bulk samples with different addition content of PSD<sub>2</sub>  $\text{Al}_2\text{O}_3$  nano-particles. The largest  $J_c$  values are recorded in the YBCO bulk sample with 0.01 wt.% of PSD<sub>2</sub>  $\text{Al}_2\text{O}_3$  nano-particles.  $J_c$  reaches  $4.7 \times 10^4 \text{ A cm}^{-2}$  under self field and  $10^4 \text{ A cm}^{-2}$  under 2 T compared to  $4 \times 10^4 \text{ A cm}^{-2}$  at 0 T and  $0.5 \times 10^4 \text{ A cm}^{-2}$  under 2 T for the reference sample. This indicates that PSD<sub>2</sub>  $\text{Al}_2\text{O}_3$  nano-particles are also effective vortex pinning centers in applied magnetic field. With further increase of PSD<sub>2</sub>  $\text{Al}_2\text{O}_3$  nano-particles amounts the critical current density decreased in the entire field range.

Comparing the  $J_c = f(\mu_0 H_a)$  curves obtained using both  $\text{Al}_2\text{O}_3$  powders characterized by two different particle size distributions, we clearly observe that in the field range <0.5 T YBCO bulk sample with 0.05 wt.% of PSD<sub>1</sub>  $\text{Al}_2\text{O}_3$  nano-particles exhibits larger  $J_c$  values compared to samples with PSD<sub>2</sub>  $\text{Al}_2\text{O}_3$  nano-particles but lower in the field range >0.5 T. On the other hand, the critical current density  $J_c$  of the pure YBCO bulk sample decreases rapidly with the applied magnetic field. However, the decreasing rate for YBCO bulk with 0.01 wt.% PSD<sub>2</sub>  $\text{Al}_2\text{O}_3$  nano-particles is lowest. These results seem that the high field performance was completely enhanced by the addition of  $\text{Al}_2\text{O}_3$  nano-particles with both particle size distributions.

A very useful tool to investigate the pinning properties in HTS materials is the volume pinning force  $F_p = J_c \times \mu_0 H_a$ . Fig. 4 shows the volume pinning force  $F_p$  as a function of the applied magnetic field at 77 K of YBCO bulk samples with different addition contents

Download English Version:

<https://daneshyari.com/en/article/8164505>

Download Persian Version:

<https://daneshyari.com/article/8164505>

[Daneshyari.com](https://daneshyari.com)